

J.K. Copper

Comparison of Annual Global Horizontal Irradiation Maps for Australia

J.K. Copper¹ and A.G. Bruce¹

¹*School of Photovoltaic and Renewable Energy Engineering, University of New South Wales,
Sydney, Australia*

E-mail: jessie.copper@unsw.edu.au

Abstract

Multiple solar irradiation maps are now available for Australia, with several maps and underlying spatial data publicly available through various web-based mapping platforms. This study aims to provide a cross comparison of the available annual global horizontal solar resource maps for Australia, highlighting regions where greater discrepancies between data sources are observed. The data sources analysed include the Australian Bureau of Meteorology (BoM) gridded solar data, MERRA-2, Meteornorm 7.2, NASA POWER, and data from Solargis and Vaisala. The methodology employed assumed that each data source had an equal weighting in the analysis. No conclusions about the accuracy of the individual data sources or which is the best data source to use are presented within this study.

The analysis highlighted high variances between the data sources across (1) the salt lake regions of South Australia and Western Australia (std ~3% to 6%); (2) the mountainous ranges of Australia (std ~3% to 8%) and (3) the National Park region of western Tasmania (std ~4% to ~14%). A band of high variance (std 2.5% to -5%) was also observed extending from central Queensland to Western Australia primarily driven by deviations observed in the Vaisala data source (-6% to -10%). MERRA-2 was also shown to overestimate annual irradiation in comparison to the other data sources, whilst a site-based analysis indicated that the bias within the Solargis dataset exhibited a linear correlation with latitude ($r = 0.90$). Outside of the aforementioned areas, the relative standard deviation in the climatology maps of annual Global Horizontal Irradiation (GHI) fell within the range of 0.5% to 2.5%. The variances observed across the available data sources highlights the importance of quantifying the uncertainty in data used for performance modelling; including annual estimates for a specific location, and the potential for using multiple data sources to provide a more robust estimate of the annual solar resource and its uncertainty.

The limitation of the results presented in this study was the lack of access to up to date long-term climatology maps from Vaisala, including the maps produced from each of Vaisala's five modelling methods.

1. Introduction

Within the solar energy industry, it is not uncommon to use a single year of weather data (i.e. a Typical Meteorology Year weather file) or a single set of annual and monthly estimates of the solar resource to undertake pre-feasibility site assessments or to produce estimates of solar energy system performance. With recent advances in deriving solar irradiance from satellite imagery, multiple solar irradiation maps and data sources are now available for undertaking resource assessment across Australia. Several of these maps and data sources are publicly available through various web mapping platforms like the Australian Renewable Energy Mapping Infrastructure (AREMI 2018), IRENA's Global Atlas for Renewable Energy (IRENA 2017), NASA's POWER data access viewer (NASA 2018) and the World Bank Group's Global Solar Atlas (The World Bank Group and Solargis 2016). These datasets differ in their spatial resolution (1° to

0.0083°), the underlying time interval (sub-hourly, hourly, 3-hourly, daily etc.), the period of data available (1980-2017, 2007-2017 etc.) and the methodology used to calculate solar irradiance. Hence, dependent on the data source/s used, different values of monthly and annual solar irradiation can arise.

Despite the prevalence of irradiation maps and data sources that are now available, there has been little analysis of the extent to which different data sources agree, or their usefulness for solar resource assessment across Australia. Such analyses have been conducted for other regions of the Globe (M. Šúri, T. Cebecauer et al. 2008, Fluri and von Backstrom 2009, M. Šúri, Cebecauer et al. 2009, Budig, Orozaliev et al. 2010) but an equivalent analysis has yet to be published for Australia. This paper aims to bridge that gap by undertaking a cross comparison between the various annual global horizontal irradiation maps and data sources which are available for Australia, including the data sources from the Australian Bureau of Meteorology (BoM), MERRA-2, Meteonorm 7.2, NASA POWER, Solargis and Vaisala.

2. Data Sources

Table 1 presents a summary of the key parameters of the six data sources analysed in this study. More detailed information from each of the data sources are presented in the following paragraphs. Given the focus of this paper is a cross comparison of the long-term annual climatologies, it is important to highlight that the length and period covered of each dataset will impact the analysis. A recent study from (Fernández Peruchena, Ramírez et al. 2016) indicated that a minimum of 11 years of GHI and 15 years of DNI data is recommended for long-term statistical characterisations. Based on this criterion the Solargis dataset (2007-2017 i.e. 11 years) only just exceeds the period recommended for the characterisation of GHI and does not yet meet the criteria for DNI. This situation will of course change over time as more years of data are captured. Although the Vaisala website indicates that 16+ years of data is available from Vaisala, the map of GHI available on the IRENA web mapping platform, which is used in this study, falls one-year shy of the 11-year requirement.

Table 1: Summary of data sources utilised in this study

Data Source	Data Type	Spatial Resolution	Period
BoM	Satellite	0.05° x 0.05° (~5km)	1990 - 2017
MERRA-2	Reanalysis	0.5° x 0.625°	1980 - 2017
Meteonorm	Interpolation between meteo stations & satellite data	Extracted at 0.5° x 0.5°; Resampled via bilinear interpolation to 0.125° x 0.125°	1991 - 2010
NASA POWER	Satellite	1.0° x 1.0° (~110km)	1984 - 2017
Solargis	Satellite	0.0083°x0.0083° (~1km)	2007 - 2016
Vaisala	Satellite	0.033° x 0.033° (~3km)	Unknown (10 years)

The **Australian Bureau of Meteorology (BoM)** publishes a variety of gridded satellite derived irradiance datasets on a spatial resolution of 0.05° x 0.05°. The hourly gridded solar radiation datasets, derived from satellite imagery, are processed by the BoM from the Geostationary Meteorological Satellites, MTSAT and Himawari-8 series operated by Japan Meteorological Agency and from GOES-9 operated by the National Oceanographic & Atmospheric Administration (NOAA) for the Japan Meteorological Agency. The hourly irradiances are then integrated over the

day to give daily solar exposure, whilst the maps of monthly and annual averages of daily global solar exposure are calculated from the daily grids (Bureau of Meteorology 2018a).

The map of average daily solar exposure (i.e. GHI) available on the Bureau's website (Bureau of Meteorology 2016) depicts the average for the period between 1990 and 2011 (22 years). Annual and monthly climatology maps of GHI and DNI from the BoM are also available on the Australian Renewable Energy Mapping Infrastructure (AREMI 2018). These maps are derived from 23 years of data for the period 1990 – 2012¹, both inclusive (Bureau of Meteorology 2018b). Given the availability of data post 2012, this study has calculated a map of annual climatology for GHI for the period between 1990 and 2017, both inclusive. The map was generated by integrating the hourly gridded satellite dataset into daily values and then calculating the annual sum and the average of the annual sums as per the methodology outlined in (Copper and Bruce 2017).

The 95% uncertainty for any of the daily exposure estimates reported by the BoM, regardless of the averaging period i.e. daily, monthly, is reported to be on the order of 3 MJ/m². The mean bias error of the hourly gridded satellite derived dataset, calculated on an annual basis across all surface sites, is reported as -1 W/m² (-0.2%)² (Bureau of Meteorology 2016). The accuracy of the hourly gridded satellite data from the BoM has also been independently assessed by a number of authors over the course of its development (Blanksby, Bennett et al. 2013, Dehghan, Prasad et al. 2014, Copper and Bruce 2015). The results from these previous analyses, and an independent analysis of the mean bias deviations, based on point comparisons with the Bureau's one-minute irradiance stations (see Table 2), indicate that the BoM's satellite derived irradiance dataset tends to underestimate irradiance for locations which experience a high proportion of clear sky conditions like Alice Springs and Learmonth and overestimates irradiance for locations with higher proportions of cloudy conditions like Darwin, Melbourne, and Cape Grim.

MERRA-2 (the second Modern-Era Retrospective analysis for Research and Applications) is a NASA atmospheric reanalysis that begins in 1980 (NASA 2017). MERRA-2 uses the Goddard Earth Observing System version 5 (GEOS-5) atmospheric model and data assimilation system (DAS). The dataset offers two-dimensional diagnostics of surface fluxes, single level meteorology, vertical integrals and land states, generated at 1 hourly, 3 hourly, daily and monthly intervals. This paper utilises the surface incident shortwave flux (SWGDN) from the single-level diagnostic `avgM_2d_rad_Nx` data product averaged over a monthly interval (NASA 2017). It should be noted that the MERRA-2 dataset is not commonly used within the Australian solar industry; however, the dataset is included within this study as the surface incident shortwave flux from MERRA-2 has been used within the solar research community (Richardson and Andrews 2014, Pfenninger and Staffell 2016, Prasad, Taylor et al. 2017).

Evaluations of MERRA's solar radiation parameters have been assessed by a number of existing studies (Kennedy, Dong et al. 2011, Wang and Zeng 2012, Zib, Dong et al. 2012, Juruš, Eben et al. 2013, Richardson and Andrews 2014, Boilley and Wald 2015, Siala and Stich 2016, Zhang, Liang et al. 2016). The consensus from these studies is that MERRA overestimates monthly mean solar irradiation when compared to surface observations. The study by (Zhang, Liang et al. 2016) included the study of monthly data from 15 Australian locations, reporting an average level of bias of 22.36 W/m². Our analysis of the datasets indicated that MERRA, on average, has a positive bias on the order of 6% when assessed against the BoM one-minute ground based irradiance stations, see Table 2, agreeing with the previous published literature from (Zhang, Liang et al. 2016). Our

¹ At the time of writing (Oct 2018), this information was not easily discernable from the AREMI 'Data Catalogue – About the Data' page.

² Based on the mean GHI and DNI values of 480 W/m² and 500 W/m² reported in the previous version of the BoM Gridded Hourly Solar Direct Normal and Global Horizontal Irradiance Metadata.

analysis indicated that the bias ranged between -2% at Broome to +17% at Melbourne, with a tendency to overestimate for all stations except Broome and Darwin.

Table 2: Normalised Mean Bias Deviations (nMBD) of Global Horizontal Irradiation, calculated with reference to the BoM One-minute Irradiance data³.

BoM Irradiance Stations	Latitude	Longitude	BoM	MERRA-2	NASA POWER	Solargis
Adelaide	-34.9524	138.5204	1.0%	5.2%	-0.9%	-1.3%
Alice Springs	-23.7951	133.889	-1.7%	5.3%	-3.3%	1.1%
Broome	-17.9475	122.2353	0.0%	-2.6%	-1.3%	1.3%
Cairns	-16.8736	145.7458	2.2%	10.1%	-1.5%	-*
Cape Grim	-40.6817	144.6892	2.6%	5.3%	4.7%	-3.9%
Cobar	-31.484	145.8294	-3.0%	5.1%	-0.9%	0.0%
Darwin	-12.4239	130.8925	4.6%	0.7%	7.7%	3.2%
Geraldton Airport	-28.8047	114.6989	-1.5%	3.0%	2.7%	-0.5%
Geraldton Airport Comparison	-28.7953	114.6975	-3.5%	3.3%	0.6%	-*
Kalgoorlie-Boulder	-30.7847	121.4533	-2.0%	8.7%	-0.9%	0.5%
Learmonth	-22.2406	114.0967	-3.5%	2.5%	-9.3%	0.3%
Longreach	-23.4397	144.2828	-1.8%	4.9%	-1.4%	0.5%
Melbourne	-37.6655	144.8321	1.8%	17.5%	3.8%	-1.6%
Mildura	-34.2358	142.0867	-2.0%	6.0%	-6.3%	-1.0%
Mt Gambier	-37.7473	140.7739	1.4%	13.1%	1.2%	-*
Rockhampton	-23.3753	150.4775	0.7%	11.2%	-1.0%	0.4%
Tennant Creek	-19.6423	134.1833	-1.0%	3.5%	-4.3%	0.8%
Townsville	-19.2483	146.7661	1.6%	7.9%	-0.8%	-*
Wagga Wagga	-35.1583	147.4575	-0.9%	6.8%	-4.1%	-0.9%
Woomera	-31.1558	136.8054	-2.9%	1.6%	-2.3%	0.4%
Average			-0.4%	5.9%	-0.9%	0.0%

-* No periods of overlapping data. For Australia, the Solargis dataset is only available from July 2006.

Meteonorm 7.2 is a software platform that can generate representative typical years for any location by interpolating between ground-based weather stations, geostationary satellites and a globally calibrated aerosol climatology (Meteotest 2017). The software can generate stochastic times series of solar radiation parameters for a typical year from the interpolated long-term monthly

³ Normalised Mean Bias Deviations (nMBD) calculated following the methodology presented in Copper, J. K. and A. G. Bruce (2015). "Assessment of the Australian Bureau of Meteorology hourly gridded solar data." *2015 Asia-Pacific Solar Research Conference, 8th - 10th Dec, Brisbane, Queensland*. using all available data from the Australian Bureau of Meteorology's one-minute ground irradiance measurement stations as of November 2018.

means. The user has the option to select between two irradiation time periods 1991-2010 and 1981-1990, for the mean monthly values or a future IPCC scenario. This study will present the results for the software's default period of 1991 to 2010.

The maps of GHI presented in this study were generated by using the Batch mode functionality of Meteonorm 7.2, providing entries of latitude and longitude coordinates for a 0.5° spatial grid. The monthly and annual values for each location were exported from Meteonorm 7.2 in text format and reconstituted back into an ascii grid. A process of bilinear interpolation was applied to the 0.5° grid of exported values to resample the data to a grid of 0.125° . Figure 4 in the appendix presents a comparison between the generated GHI map from this study against the publicly available map (spatial resolution of 0.125°) of annual GHI published on Meteonorm's website.

The reported uncertainty of Meteonorm 7.2 for GHI is 3 to 9%. Based on Figure 8.4.3 of the Meteonorm 7.2 Handbook part II: Theory (Meteotest 2017), higher uncertainties are reported across the centre of Australia. A map of the uncertainty of GHI was also generated based on the values reported for each grid location exported from the software. This map is published in Figure 5 within the appendix, in conjunction with a map depicting the 'Share of satellite data' used in the interpolation process. Figure 5 highlights how the reported GHI uncertainty is directly correlated to the share of satellite data used in the interpolation process. It should be noted that the reported uncertainties from Meteonorm are combined uncertainties accounting for (1) the ground measurements (the uncertainty of the measurement itself and the long-term variability i.e. interannual variability of the local climate); (2) the interpolation process; and (3) splitting GHI into its diffuse and direct components. It should also be noted that the Meteonorm dataset was not included in the bias analysis presented in Table 2, as the Meteonorm software generates representative typical years, rather than actual years of weather data.

The **NASA POWER** data was obtained from the NASA Langley Research Center (LaRC) POWER Project funded through the NASA Earth Science/Applied Science Program (NASA 2018). The POWER data set consists of two categories of data; solar and meteorological. The NASA POWER dataset is included in this study as numerous PV modelling packages provide access to this data source. The POWER solar data is inferred via radiative transfer models from satellite observations and is taken from NASA's Global Energy and Water Exchange Project/Surface Radiation Budget (GEWEX SRB) and NASA's Fast Longwave And Shortwave Radiative (FLASHFlux) projects (P.W. Stackhouse, T. Zhang et al. 2018). The data is initially produced on 3-hourly time increments which are averaged to provide daily values. The daily average values are used to calculate climatologically averaged monthly values. The climatology dataset, which includes both GHI and DNI covers the period of July 1983 to June 2005. However, additional data for GHI can be obtained up to near real time. Hence, for GHI the period 1984 to 2017 is analysed in this study.

The accuracy of the solar data has been evaluated by NASA through direct comparison with surface site observations from the Baseline Surface Radiation Network (BSRN). The time series of solar data available from the POWER archive are taken from various models over the period 1983 to near real time. Details of the accuracy for each period and model are presented in (P.W. Stackhouse, T. Zhang et al. 2018). The published figures of bias for the daily mean short wave (SW) radiation all sky conditions for the 60° Equatorward analysis are: -1.13% for the GEWEX SRB project (July 1983 – 2007); -0.74% for FLASHFlux v2 (D, E, G, H) (2008 – 2012); and -1.86% for FLASHFlux v3 (A, B, C) (2013 – near real time). Hence, the general conclusion is that the NASA POWER dataset on average underestimates the daily mean values of irradiation. Our analysis of the NASA POWER dataset (see Table 2) also confirms this general conclusion. However, the average figures mask how the NASA POWER dataset also tends to underestimate irradiation for locations which experience a high proportion of clear sky conditions and overestimate for locations with higher proportions of cloudy conditions.

It should be noted that the POWER methodology document (P.W. Stackhouse, T. Zhang et al. 2018) contains a note stating that the *'time series of daily surface insolation may include multiple data sources; accordingly, it is not recommend for use in assessing climate trends that encompass a source data change'*.

Solargis is a third-party provider of satellite derived solar resource data including time series data (historical and forecast), geospatial maps and TMY and P90 weather files. Solargis calculates GHI via the SOLIS clear-sky model based on inputs of Atmospheric Optical Depth (AOD) derived from the global MACC-11 database; water vapour derived from CFSR and GFS databases; and a constant value for Ozone. Cloud attenuation of the SOLIS clear-sky profile is undertaken via the means of a cloud index derived from the relationship of radiance at the Earth's surface, recorded by meteorological geostationary satellites in several spectral channels, with the cloud optical transmittance (Solargis 2016).

Annual maps of Solargis data can be obtained from the World Bank Group's Global Solar Atlas (The World Bank Group and Solargis 2016). For the region of Australia, the publicly available maps cover the period 2007 to 2015, both inclusive. In addition to the publicly available data, maps of annual GHI were obtained from Solargis covering the period 2007 to 2016, both inclusive. The accuracy of the solar data has been evaluated by Solargis through direct comparison with surface site observations from more than 200 sites across the globe, including 11 of the BoM ground-based irradiance stations. The results of our assessment (see Table 2) of the Solargis dataset tends to agree with the published validation statistics for the Australian locations (Solargis 2016), highlighting that bias within the Solargis dataset has a strong correlation with latitude (Pearson correlation coefficient of 0.92 and 0.9, respectively for absolute and normalised mean bias deviations).

Vaisala is another third-party provider of satellite derived solar resource data including time series data and geospatial maps. Vaisala calculates GHI via five separate modelling methods which differ in the underlying clear sky model (modified Kasten, REST2); AOD data source (MODIS Dark Target, MODIS Deep Blue) and resolution (monthly, daily); and turbidity inputs (ECMWF-MACC, MERRA2) (Vaisala 2018a). As per the SolarGIS method, GHI is calculated by combining the outputs of the clear-sky model with cloud index values calculated from satellite imagery.

The Vaisala annual map of GHI was obtained from the IRENA (International Renewable Energy Agency) Global Atlas for Renewable Energy (IRENA 2017). Unfortunately, the exact version and period of the Vaisala dataset used to generate the GHI map published on the IRENA Global Atlas is unknown as the metadata links on the website are broken. Our best guess is that this dataset covers a 10 year period between 1999 and 2010 using the Vaisala 1.0 solar algorithms, as per the documentation on Vaisala's Support webpage for their own Solar Online Tools (Vaisala 2018b). The accuracy of Vaisala's solar data has been evaluated by Vaisala through direct comparisons with surface site observations from 196 stations across the globe, including 19 locations across Australia. The regional statistics for the Vaisala 1.0 model across East Asia and Oceania indicated a relative mean bias error of -0.49% (Vaisala 2018a). Although the exact statistics for each individual site are not reported, a figure of coloured mean bias dot points on a map of East Asia and Oceania indicates that the v1.0 model tends to achieve significantly higher levels of negative bias for Australia (excluding Darwin and Melbourne with positive bias) than is indicated by the -0.49% average across East Asia and Oceania. Analysis undertaken by (Smith 2018) also indicates that the Vaisala v1.0 model tends to on average underestimate GHI in comparison to the BoM and Solargis datasets.

The major limitation of the results presented in this study is the lack of access to up to date long-term climatology maps and the underlying data from Vaisala, including the maps produced from each of Vaisala's five modelling methods. Hence, an independent assessment of the bias of the Vaisala dataset was unable to be included within this current study.

3. Methodology and Results

The maps from all data providers were resampled via data replication⁴ to a spatial resolution of 0.0083° to correspond to the Solargis dataset. The alternative method is to aggregate⁵ the maps to a spatial resolution of 0.5° to correspond to the NASA POWER and MERRA-2 datasets. The results of this alternative method are presented within the Appendix. Resampling was undertaken to facilitate the calculation of the mean and absolute standard deviation of the available datasets. The maps of relative standard deviation were then calculated as the standard deviation divided by the mean multiplied by 100 to convert the values to percentages. The methodology employed in this study assumed that each data source had an equal weighting in the analysis. An equal weighting was applied as we did not want to make any preconceptions of the performance of each data source. However, as discussed above the data sources are not equal, they vary in period of data available (10 to 38 years), spatial resolution ($\sim 1\text{km}$ to 110km) and accuracy/bias of the underlying method to calculate GHI. Uncertainty in the mean estimate could be reduced by weighting each of the data sources by the afore listed factors.

Figure 1 presents the individual maps of annual GHI, whilst Figure 2 presents the mean and relative standard deviations of the maps in Figure 1, excluding MERRA-2. Relative differences of each dataset to the mean of the datasets are presented in Figure 3. The MERRA-2 dataset is excluded from the mean and standard deviation calculations, as this dataset is not commonly used within the Australian solar industry and previous studies and the mean bias statistics presented in Table 2 indicate that MERRA-2 overestimates solar radiation. MERRA-2 is however included in the visual comparisons of Figure 1 and Figure 3 as this dataset has been used in the research community (Richardson and Andrews 2014, Pfenninger and Staffell 2016, Prasad, Taylor et al. 2017).

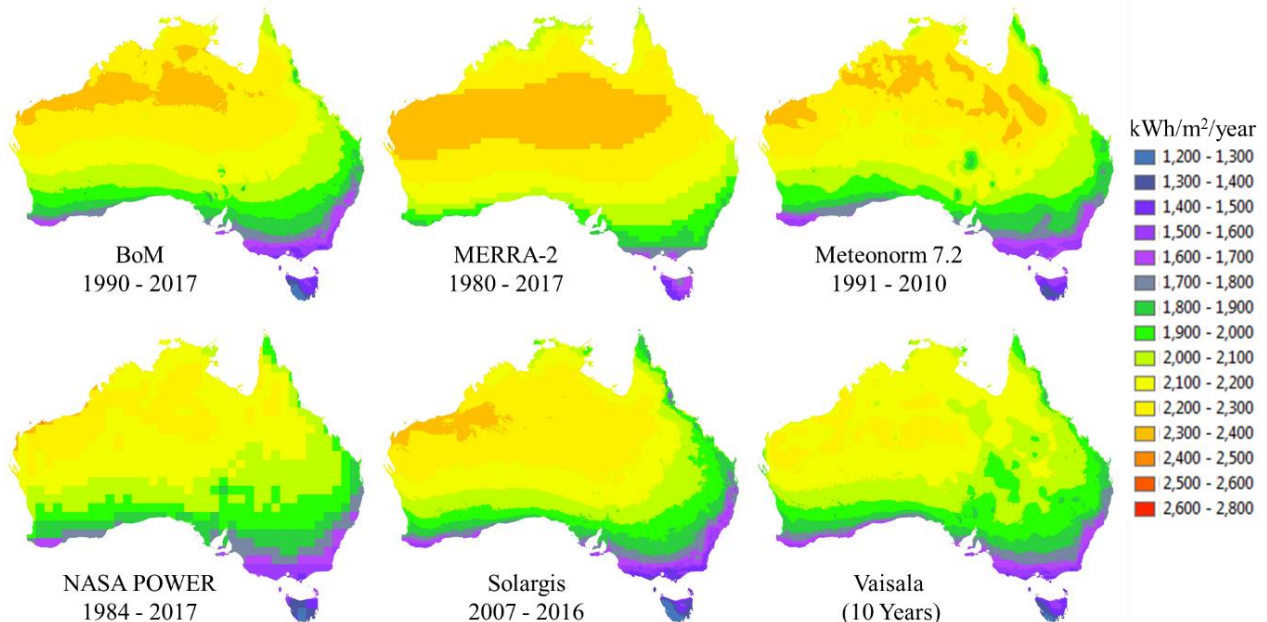


Figure 1: Visual comparison of annual Global Horizontal Irradiance in $\text{kWh/m}^2/\text{year}$

⁴ Each output cell of the resampled 0.0083° map is identical to the value of the input cell of the original map which encompassed the extent of the output cell i.e. the same value would be extracted from both maps.

⁵ Each output cell of the aggregated 0.5° map contains the mean of the input cells of the original map that are encompassed by the extent of the output cell. i.e. the lower resolution 0.5° map is a spatial average of the higher resolution map.

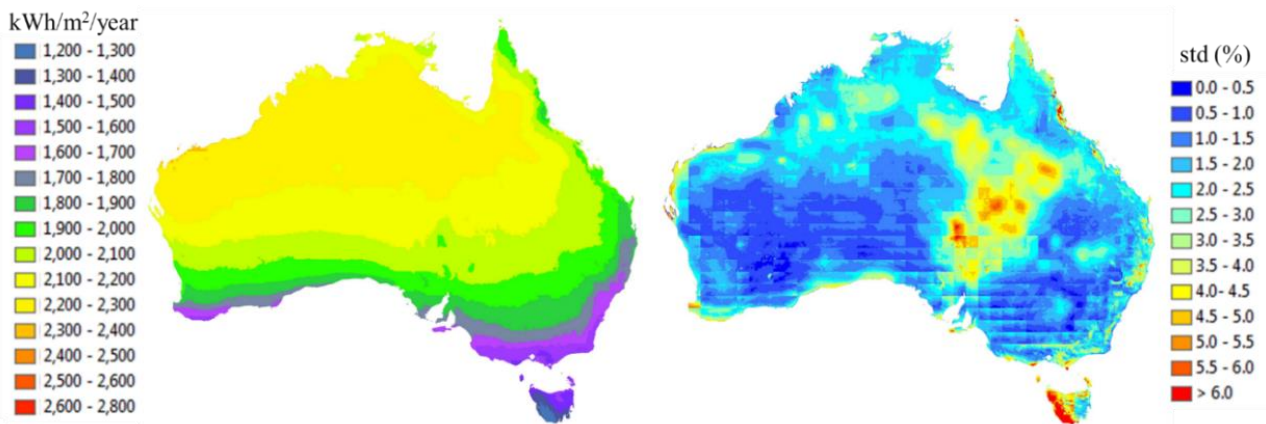


Figure 2: Mean (left) and relative standard deviation (right) of the annual GHI maps presented in Figure 1, excluding MERRA-2

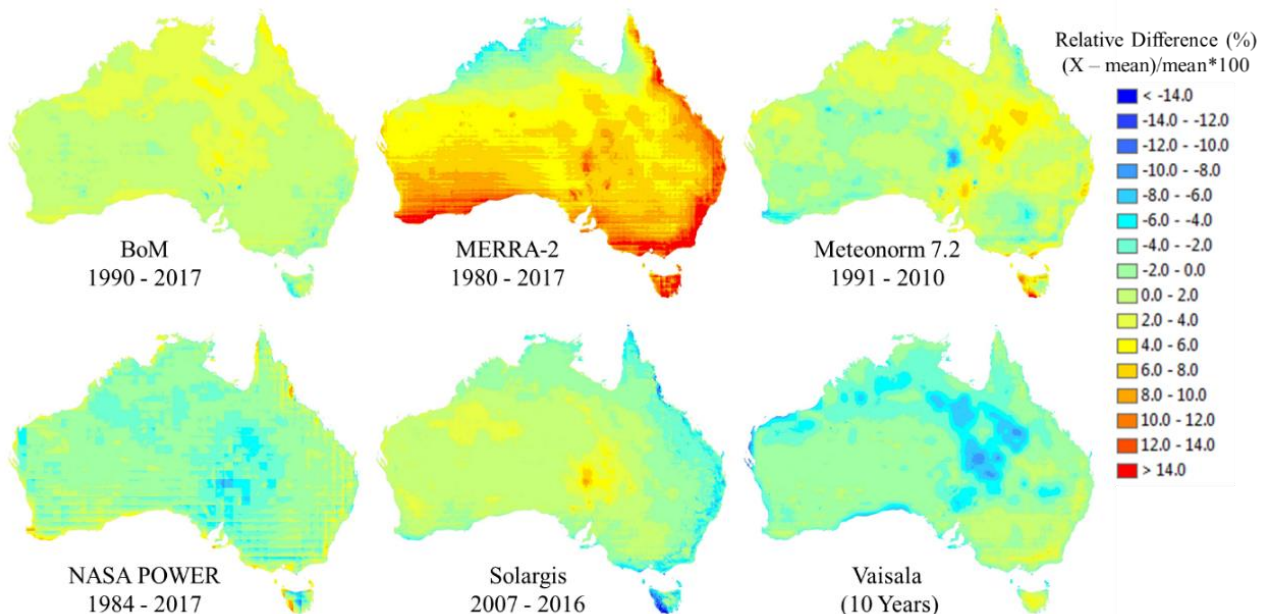


Figure 3: Relative difference between each GHI dataset and the mean of the datasets presented in Figure 2.

Figure 1 and Figure 3 confirm that MERRA-2 primarily overestimates annual GHI on the order of 4% to >14%, when compared to the mean of the other datasets. The exception is for the top end region of the Northern Territory where the MERRA-2 dataset slightly underestimates on the order of 0 to -3%. These results agree with our site-based analysis of the MERRA-2 dataset which indicated that the bias ranged between -2% at Broome to +17% at Melbourne, with a tendency to overestimate for all stations except Broome and Darwin. Figure 1 also reveals the spatial limitations of the MERRA-2 (0.5°x0.625°) and NASA POWER (1°x1°) datasets when compared against the other four datasets available. The spatial resolution of the NASA POWER dataset is also the cause of the grid pattern which appears in the relative standard deviation map presented in Figure 2.

The map of relative standard deviation presented in Figure 2, indicates that the largest differences between the available GHI datasets occurs across (1) the salt lake regions of South Australia (std ~ 6%) (2) a band spanning from central Queensland to Western Australia (std ~3% to 6%); (3)

along the mountain ranges of Australia (std ~ 4% to 6%) and (4) across the National Park regions in Tasmania (std ~ 4% to >14%). Outside of these regions the relative standard deviation in the climatology maps of annual GHI fall within the range of 0.5% to 2.5%, excluding MERRA-2. Similar observations can be drawn from the alternative analysis presented in Figure 6 in the appendix, which used the 0.5° aggregated maps as input into the mean and standard deviation analysis.

The driver of the observed differences across the salt lake regions of South Australia is due to the inability of the various satellite derived irradiance datasets to distinguish between cloud cover and high levels of reflectance off the salt lakes. This phenomenon is most pronounced over the regions of Lake Eyre, Lake Torrens and Lake Frome and is most evident in the BoM, Meteonorm 7.2, NASA and Vaisala datasets. Regions of high variability for the salt lakes across the Gibson Desert in Western Australia, Lake Mackay and Lake Disappointment, were also observed but not to the same degree of variation as those in South Australia. The Solargis dataset is not immune to this phenomenon, however the annual map of GHI indicates that this dataset does a better job at distinguishing between cloud cover and salt lakes. The map of the relative differences of the Solargis data to the mean of the datasets in Figure 3, indicates that the Solargis map deviates on the order of 6% to 8% across the salt lake region in South Australia. Here, this deviation is not an artefact of the Solargis dataset but rather reflects how the BoM, Meteonorm 7.2, NASA and Vaisala datasets underestimate the long-term annual irradiation across this region.

The region of high relative standard deviation across south-east and central Queensland is driven by higher levels of annual irradiation in the Meteonorm 7.2 (4% to 7%) dataset in combination with below average levels from the Vaisala (-6% to -10%) dataset, see Figure 3. The exact causes of the higher differences between the two datasets, across these regions, are unknown. Further the band of higher differences observed across northern Western Australia and central Northern Territory are again caused by the lower values from the Vaisala dataset in comparison to the other datasets for this region. This can best be observed by comparing the pattern of high relative standard deviation in Figure 2, to the map of relative differences of the Vaisala dataset to the mean of the datasets, as presented in Figure 3. Although the exact site based statistics from Vaisala's in-house validation are unknown, the map of coloured-dot points presented in their validation paper for East Asia and Oceania indicated that the v1.0 model has a negative level of bias for all sites except Darwin and Melbourne (Vaisala 2018a). The map of relative differences presented in Figure 3 appears to agree with the published site-based statistics for Vaisala's v1.0 model.

The observed differences across the mountainous regions of the maps is driven by the higher spatial resolution of the Solargis dataset (0.0083°x0.0083°). Theoretically, the Solargis dataset better resolves the influence of horizon shading⁶, when compared against the other lower spatial resolution datasets. This is most evident when comparing Solargis to the NASA POWER (1°x1°) dataset i.e. the comparison of the spatial average of irradiation over a grid of approx. 1km vs. 110 kms. The spatial resolution of the Vaisala (~3km) and BoM (~5km) datasets also contribute to the variability observed across the mountainous regions, where changes in annual irradiation between nearby locations can vary significantly within a few kilometres due to differences in horizon shading.

The largest differences observed across the datasets occurs over the National Park regions of western Tasmania (std 4% to > 14%). In comparison to the mean of the datasets, Solargis provides the lowest estimate and Meteonorm 7.2 the highest for this region (excluding MERRA-2). The published site based statistics from Solargis (Solargis 2016) and the bias statistics presented in Table 2, indicate that Solargis underestimates the level of irradiance for the location of Cape

⁶ Meteonorm 7.2 also has functionality to incorporate horizon shading. The maps presented in this paper do not correctly reflect this functionality of Meteonorm as the maps were generated using a spatial resolution of 0.5°x0.5° resampled via bilinear interpolation to a grid of 0.125°x0.125°.

Grim, which is located within the north-western region of Tasmania, on the order of 4% whilst the BoM, MERRA-2 and NASA POWER datasets all overestimate irradiation for this location. Hence, for the Solargis dataset there appears to be agreement between the negative deviations observed across Tasmania in Figure 3 and the published point-based statistics for this data source.

Finally, when comparing the maps of relative differences, Figure 3 indicates that the map of annual GHI from the BoM tends to display the lowest range of deviations from the mean of the data sources, followed by the Solargis data source. The reasons for the higher deviations observed in the Solargis data source, are partially a reflection of the limitations in the other data sources, i.e. the salt lakes in South Australia and lower spatial resolutions, whilst also reflecting the latitude dependence of the bias within the Solargis dataset. Similarly, it should also be reiterated that the Solargis data source is currently limited in the period of data available (2007 to near real time), and based on recent research from (Fernández Peruchena, Ramírez et al. 2016), the data source only just meets the minimum of 11 years of data recommended for long-term statistical characterisation of GHI and does not yet meet the 15 year recommendation for DNI.

4. Conclusions

This study undertook a cross comparison of the annual global horizontal irradiation data sources available for Australia. The methodology employed assumed that each data source had an equal weighting in the analysis. The analysis of the annual climatologies indicated that a number of the data sources have limitations across (1) the salt lake regions of South Australia and Western Australia; (2) the mountainous regions of Australia (std ~3% to 8%); and (3) the National Park regions of western Tasmania (std ~4% to ~14%). A band of high variation (-6% to -10%) was also observed across central Queensland, extending across to Western Australia, primarily driven by below average values from the Vaisala dataset. For GHI, MERRA-2 was also shown to significantly overestimate annual GHI, whilst the bias within the Solargis dataset was found to exhibit a linear correlation with latitude. Outside of the aforementioned areas the relative standard deviation in the climatology maps of annual GHI fell within the range of 0.5% to 2.5%. Published validation statistics for the various datasets also appeared to agree with the maps of relative differences to the mean of the data source presented in this study. This highlights the potential of using multiple data sources to provide a more robust estimate of the annual solar climatology and a measure of the uncertainty of the estimate.

One of the limitations of this study was the lack of up to date long-term climatology maps from Vaisala, including maps produced from each of Vaisala's five modelling methods. Future work will aim to incorporate these datasets as well as an independent assessment of the site-based statistic for each data source. Future work will also expand this analysis to include results for DNI and interannual variability.

Appendix:

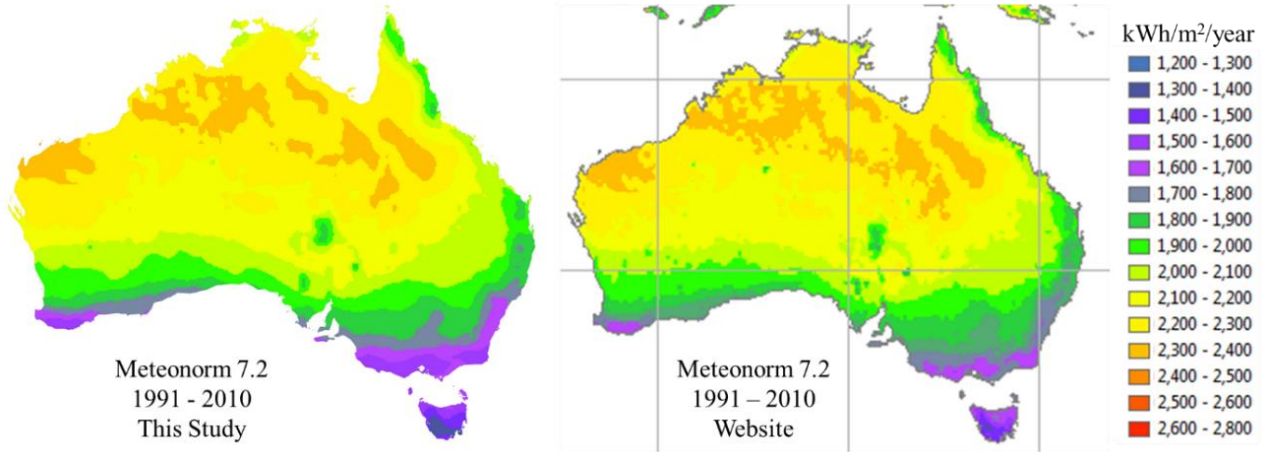


Figure 4: Visual comparison between the GHI Meteororm 7.2 map generated for this study versus the publicly available map for version 7.2 from Meteororm's website.

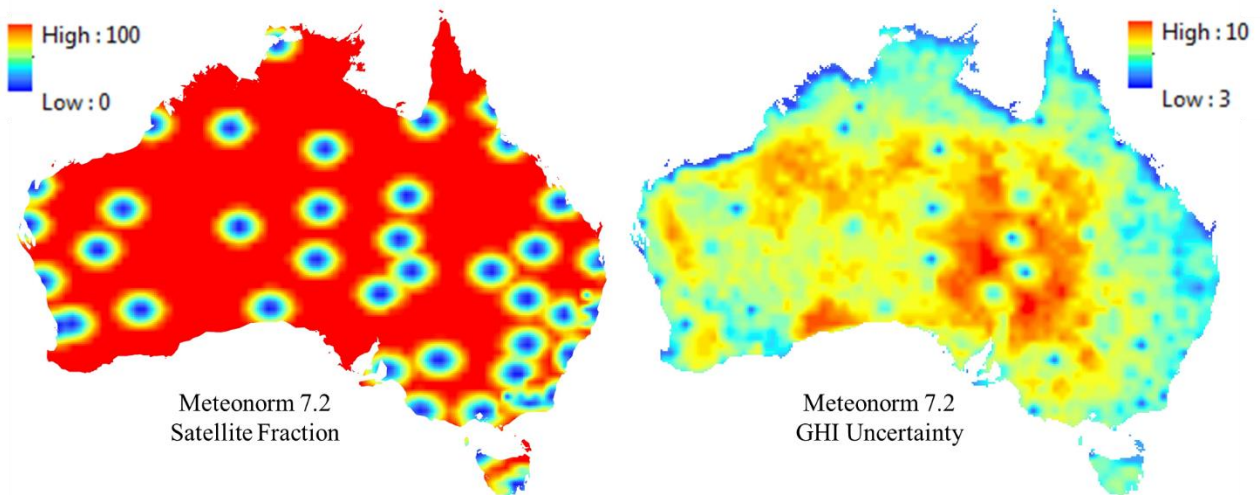


Figure 5: Map of the 'Share of satellite data' used in the interpolation process (left) and the uncertainty of the yearly GHI value (right) as reported in the Meteororm 7.2 output files.

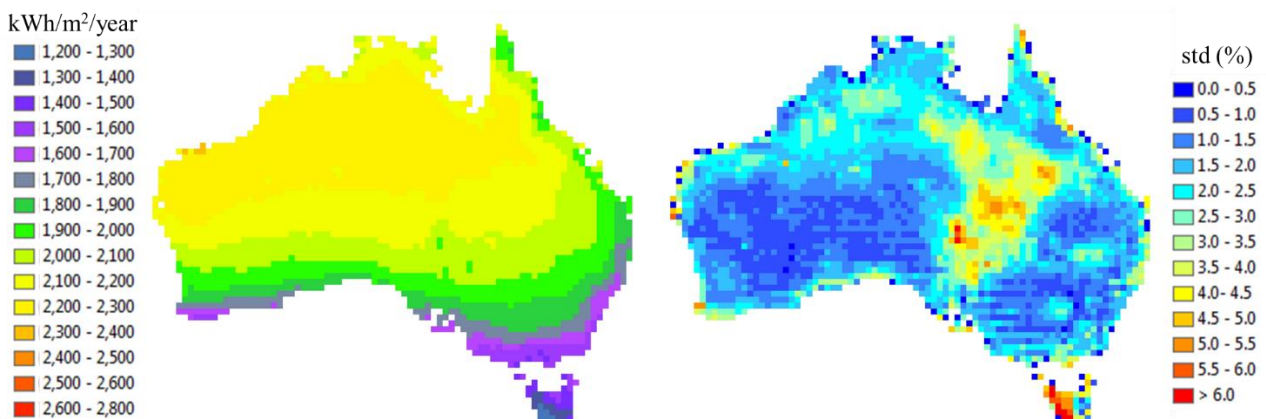


Figure 6: Mean (left) and relative standard deviation (right) of the annual GHI maps which were resampled to a spatial resolution of 0.5°x0.5°, excluding MERRA-2

References

- AREMI. (2018). "Australian Renewable Energy Mapping Infrastructure." Retrieved 10/10/2018, from <http://nationalmap.gov.au/renewables/>.
- Blanksby, C., D. Bennett and S. Langford (2013). "Improvement to an existing satellite data set in support of an Australia solar atlas." Solar Energy **98, Part B(0)**: 111-124.
- Boilley, A. and L. Wald (2015). "Comparison between meteorological re-analyses from ERA-Interim and MERRA and measurements of daily solar irradiation at surface." Renewable Energy **75**: 135-143.
- Budig, C., J. Orozaliev and K. Vajen (2010). Comparison of different sources of meteorological data for Central Asia and Russia. EUROSUN,, Graz, Autriche.
- Bureau of Meteorology. (2016). "Gridded Hourly Solar Direct Normal and Global Horizontal Metadata." Retrieved 20/06/2016, from http://www.bom.gov.au/climate/data-services/docs/IDCJAD0026_metadata_gridded_hourly_GHI.pdf
http://www.bom.gov.au/climate/data-services/docs/IDCJAD0027_metadata_gridded_hourly_DNI.pdf.
- Bureau of Meteorology. (2016, November 2016). "Maps - Average Conditions: Average Daily Solar Exposure." Commonwealth of Australia, 2018, from http://www.bom.gov.au/jsp/ncc/climate_averages/solar-exposure/index.jsp.
- Bureau of Meteorology. (2018a). "Australian Gridded Solar Climatology Web Data Services." Commonwealth of Australia Retrieved 10/10/2018, from <http://www.bom.gov.au/metadata/catalogue/view/ANZCW0503900428.shtml>.
- Bureau of Meteorology. (2018b). "Daily Solar Radiation Model Description." Commonwealth of Australia, 2018, from <http://www.bom.gov.au/climate/austmaps/about-solar-maps.shtml>.
- Copper, J. K. and A. Bruce. (2017). "Interannual Variability of the Solar Resource across Australia." from <http://apvi.org.au/solar-research-conference/proceedings-apsrc-2017/>.
- Copper, J. K. and A. G. Bruce (2015). "Assessment of the Australian Bureau of Meteorology hourly gridded solar data." 2015 Asia-Pacific Solar Research Conference, 8th - 10th Dec, Brisbane, Queensland.
- Dehghan, A., A. A. Prasad, S. C. Sherwood and M. Kay (2014). "Evaluation and improvement of TAPM in estimating solar irradiance in Eastern Australia." Solar Energy **107(0)**: 668-680.
- Fernández Peruchena, C. M., L. Ramírez, M. A. Silva-Pérez, V. Lara, D. Bermejo, M. Gastón, S. Moreno-Tejera, J. Pulgar, J. Liria, S. Macías, R. Gonzalez, A. Bernardos, N. Castillo, B. Bolinaga, R. X. Valenzuela and L. F. Zarzalejo (2016). "A statistical characterization of the long-term solar resource: Towards risk assessment for solar power projects." Solar Energy **123**: 29-39.
- Fluri, T. P. and T. W. von Backstrom (2009). Comparison of solar resource assessments for South Africa. ISES Solar World Conference, . Johannesburg, South Africa.
- IRENA. (2017). "Global Atlas for Renewable Energy v3.0." International Renewable Energy Agency Retrieved 21/11/2017, from <https://irena.masdar.ac.ae/>.

- Juruš, P., K. Eben, J. Resler, P. Krč, I. Kasanický, E. Pelikán, M. Brabec and J. Hošek (2013). "Estimating climatological variability of solar energy production." Solar Energy **98, Part C(0)**: 255-264.
- Kennedy, A. D., X. Dong, B. Xi, S. Xie, Y. Zhang and J. Chen (2011). "A Comparison of MERRA and NARR Reanalyses with the DOE ARM SGP Data." Journal of Climate **24(17)**: 4541-4557.
- M. Šúri, T. Cebecauer, P. Ineichen, J. Remund, C. Hoyer-Klick, T. Huld, D. D and P. W. J. Stackhouse (2009). Comparison of Direct Normal Irradiation Maps for Europe. SolarPACES Conference, Berlin Germany.
- M. Šúri, T. Cebecauer, P. Blanc, J. Remund, T. Huld and D. Dumortier (2008). First Steps in the Cross-Comparison of Solar Resource Spatial Products in Europe. EUROSUN, Lisbon, Portugal.
- Meteotest. (2017). "Meteonorm - Handbook part II: Theory." Retrieved 10/10/2018, from http://www.meteonorm.com/images/uploads/downloads/mn72_theory7.2.pdf.
- NASA. (2017). "README Document for MERRA2 Data Products." Retrieved 10/10/2018, from <https://gmao.gsfc.nasa.gov/reanalysis/MERRA/>.
- NASA. (2018). "Power Project Data Sets." Retrieved 12/11/2018, from <https://power.larc.nasa.gov/index.php#ack>.
- P.W. Stackhouse, T. Zhang, D. Westber, A.J. Barnett, T. Bristow, B. Macperson and J. M. Hoell. (2018). "POWER Release 8 (with GIS Applications) Methodology (Data Parameters, Sources & Validation)." Retrieved 10/10/2018, from https://power.larc.nasa.gov/documents/POWER_Data_v8_methodology.pdf.
- Pfenninger, S. and I. Staffell (2016). "Long-term patterns of European PV output using 30 years of validated hourly reanalysis and satellite data." Energy **114**: 1251-1265.
- Prasad, A. A., R. A. Taylor and M. Kay (2017). "Assessment of solar and wind resource synergy in Australia." Applied Energy **190**: 354-367.
- Richardson, D. B. and R. W. Andrews (2014). Validation of the MERRA dataset for solar PV applications. 2014 IEEE 40th Photovoltaic Specialist Conference (PVSC).
- Siala, K. and J. Stich (2016). "Estimation of the PV potential in ASEAN with a high spatial and temporal resolution." Renewable Energy **88**: 445-456.
- Smith, C. (2018). "Validation of satellite irradiance data with trusted ground based measurements - Assessing the uncertainty in irradiance predictions." Clean Energy Council, Large-Scale Solar Industry Forum, from <https://www.cleanenergycouncil.org.au/dam/cec/events/sif-2018/Presentations/chris-smith-sif-18.pdf>.
- Solargis. (2016). "Solargis Solar Resource Database: Description and Accuracy." Retrieved 15/07/17, from <http://solargis.com/assets/doc/Solargis-database-description-and-accuracy.pdf>.
- The World Bank Group and Solargis. (2016). "Global Solar Atlas." Solar resource data obtained from the Global Solar Atlas, owned by the World Bank Group and provided by Solargis Retrieved 21/11/2017, from <http://globalsolaratlas.info/>.

Vaisala. (2018a). "Vaisala 3TIER Services Global Solar Dataset: Methodology and Validation." Retrieved 10/10/2018, from <https://www.vaisala.com/sites/default/files/documents/3TIER%20Solar%20Dataset%20Methodology%20and%20Validation.pdf>.

Vaisala. (2018b). "Vaisala Energy Support - Solar Online Tools - What solar values are shown on the map?" Retrieved 15/10/2018, from <https://www.3tier.com/en/support/solar-online-tools/what-solar-values-are-shown-map/>.

Wang, A. and X. Zeng (2012). "Evaluation of multireanalysis products with in situ observations over the Tibetan Plateau." Journal of Geophysical Research: Atmospheres **117**(D5): n/a-n/a.

Zhang, X., S. Liang, G. Wang, Y. Yao, B. Jiang and J. Cheng (2016). "Evaluation of the Reanalysis Surface Incident Shortwave Radiation Products from NCEP, ECMWF, GSFC, and JMA Using Satellite and Surface Observations." Remote Sensing **8**(3): 225.

Zib, B. J., X. Dong, B. Xi and A. Kennedy (2012). "Evaluation and Intercomparison of Cloud Fraction and Radiative Fluxes in Recent Reanalyses over the Arctic Using BSRN Surface Observations." Journal of Climate **25**(7): 2291-2305.